J. Fluid Mech. (2006), *vol.* 560, *pp.* 395–414. © 2006 Cambridge University Press
doi:10.1017/S002211200600067X Printed in the United Kingdom

Rayleigh–Taylor problem for a liquid–liquid phase interface

By XUEMEI CHEN AND ELIOT FRIED

Department of Mechanical and Aerospace Engineering, Washington University in St Louis, St Louis, MO 63130-4899, USA

(Received 3 October 2005 and in revised form 16 January 2006)

A linear stability analysis of the Rayleigh–Taylor problem for an incompressible fluid undergoing a liquid–liquid phase transformation is presented. Both inviscid and linearly viscous fluids are considered and interfacial tension is taken into account. Instability is possible only when the phase with the higher density is above that with the lower density. Study of the inviscid case shows that the exchange of mass between the phases decreases significantly both the range of unstable wavenumbers and the maximum growth rate for unstable perturbations as compared to those arising classically. For a linearly viscous fluid, the shear and dilational viscosities of the interface are taken into account as are the migrational viscosities associated with the motion of the interface relative to the underlying fluid. When no mass exchange occurs between the phases in the base state and the interfacial viscosities are neglected, the growth rates exceed by at least an order of magnitude those for the classical Rayleigh–Taylor problem. The various interfacial viscosities slow the growth rates of disturbances, but do not influence the range of unstable wavenumbers. For both the inviscid and viscous cases, interfacial tension plays the same stabilizing role as it does classically.

1. Introduction

A single-component fluid may exist in more than one isotropic liquid phase (Angell 1995). A process in which one such phase grows at the expense of another is called a 'liquid–liquid phase transformation'. Experimental evidence indicates that liquid–liquid phase transformations occur in a variety of substances. Aasland & McMillan (1994) reported a density-driven liquid–liquid phase transformation in a supercooled melt of Al_2O_3–Y_2O_3. Togaya (1997) and Glosli & Ree (1999) studied high-pressure liquid–liquid phase transformations in carbon. Katayama *et al.* (2000) used in *situ* X-ray diffraction to establish the existence of a first-order liquid–liquid phase transformation in phosphorus. From the theoretical perspective, Kurita & Tanaka (2005) argued that liquid–liquid phase transformations are possible in various molecular liquids, which – owing to anisotropic interactions associated with hydrogen bonding – have a tendency to form long-lived locally-favoured structures. Although evidence of such transformations has emerged only relatively recently, their importance in various chemical engineering processes is well-recognized (Tanaka 2000; Lee & Swendsen 2001; Rzehak, Müller-Krumbhaar & Marquardt 2003). An example of a process designed to take advantage of a transformation between two liquid phases is provided by hetergenerous azeotropic distillation (Widagdo & Seider 1996), where the transformation facilitates separation. Liquid–liquid phase transformations may also occur as undesired side-effects during vapour- or gas-liquid unit operation.

https://doi.org/10.1017/S002211200600067X Published online by Cambridge University Press

Typical examples are provided by condensation (Burghardt & Bartelmus 1994), boiling heat transfer (Troniewski *et al.* 2001), mass transfer in falling film devices, and distillation in trays or packed columns (Siegert *et al.* 2000). In these examples, liquid–liquid phase transformations may seriously undermine the efficiency of the intended operations (Rzehak *et al.* 2003).

Despite the scientific and technological importance of liquid–liquid phase transformations, questions concerning the hydrodynamic stability of an interface separating the two liquid phases undergoing transformation do not appear to have been addressed prior to this work.

Hydrodynamic stability has been recognized as one of the central issues of fluid mechanics for more than a century. It has applications to engineering design, to meteorology and oceanography, and to astrophysics and geophysics. When a heavy fluid is superposed over a light fluid in a gravitational field and surface tension is neglected, the interface between the fluids is catastrophically unstable. Any perturbation of the interface tends to grow with time, producing the phenomenon known as Rayleigh–Taylor instability.

Rayleigh (1900) and Taylor (1950) considered the case of two incompressible fluids and predicted this instability by means of linear analysis that took into account the effects of inertial and body forces. The exponential growth rate determined by such treatment is proportional to $\sqrt{k}$, with k being the wavenumber of the perturbation. The experimental studies of Lewis (1950) showed that, for an liquid–air interface, this prediction was nearly correct during the initial phase of the instability. Linearized stability analyses were later extented to include the effects of surface tension, viscosity and spatially non-uniform density distributions during the initial stage of the instability. Bellman & Pennington (1954) studied the effect of surface tension and found the cutoff wavenumber k_{c} below which perturbations are unstable, to be

$$k_{\mathrm{c}} = \sqrt{\frac{(\varrho^{+} - \varrho^{-})g}{\gamma}}, \tag{1.1}$$

where ϱ^{+} and ϱ^{-} denote the constant densities of the fluids above and below the interface, g is the magnitude of acceleration due to gravity, and γ is the surface tension. When surface tension is neglected, the system is unstable whenever $\varrho^{+} > \varrho^{-}$. However, when surface tension is taken into account, the system is linearly stable provided that $k > k_c$. Still when k is sufficiently small, or the wavelength is sufficiently long, the equilibrium system is unstable if the heavier fluid is on top of the lighter fluid. The cutoff wavenumber defined by (1.1) is unchanged when viscous effects are taken into account. In particular, Chandrasekhar (1955, 1961) provides an expression for the variation of the linear growth rate with both the Reynolds number Re and the Atwood number,

$$At = \frac{\varrho^{+} - \varrho^{-}}{\varrho^{+} + \varrho^{-}}, \tag{1.2}$$

both without and with surface tension.

So far, studies of interfacial instability have been limited to the case where the interface separating the two fluids is a material surface. In this case, there is no transfer of mass across the interface. Thermal effects often play only a secondary role; therefore, the effect of heat transfer had also been neglected for the classical Rayleigh–Taylor problem. However, there are situations when the effect of mass or heat transfer across the interface are essential in determining the flow field. Hsieh (1978) presented a simple formulation to deal with interfacial instability problems involving mass and

https://doi.org/10.1017/S002211200600067X Published online by Cambridge University Press

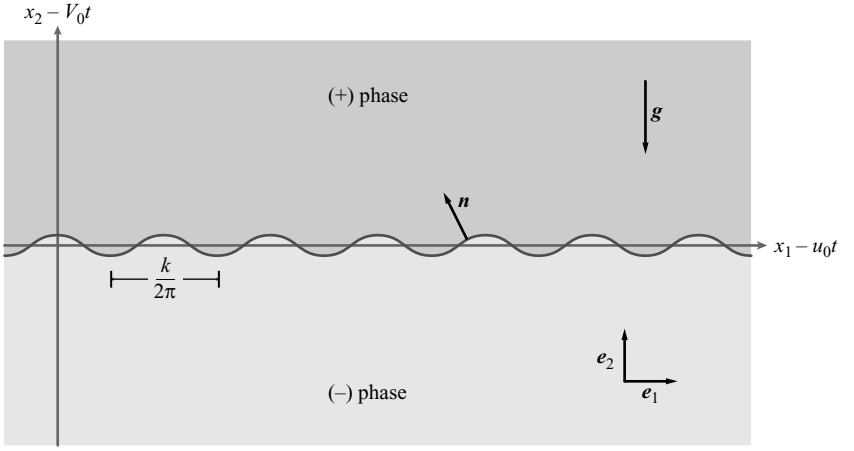


FIGURE 1. Schematic of the (+) and (−) phases and the disturbed interface.

heat transfer. For an inviscid liquid–vapour system, he found that the effects of mass and heat transfer tend to enhance the stability of the system when the vapour is hotter than the liquid, although the classical stability criterion is still valid. Later authors such as Higuera (1987) studied the hydrodynamic stability of an evapourating liquid including the effect of fluid viscosities. He employed the classical Hertz–Knudsen–Langmuir equation (Hertz 1882; Knudsen 1915; Langmuir 1916) to connect the mass flux with the thermodynamic conditions at the interface. The destabilizing effects of the perturbations of gas pressure and vapourizing mass flux, previously pointed out by Plesset & Prosperetti (1982) in inviscid fluids, were recovered in a slightly more general setting, and their competition with the stabilizing effects of gravity and surface tension led to a stability limit.

In parallel with work on hydrodynamic stability, an extensive literature has developed concerning the morphological stability of phase interfaces. Mullins & Sekerka (1963) considered a spherical particle growing into a supersaturated solution and stability of the planar front during directional solidification of a binary liquid. In investigating the evolution of small perturbations of the interface, Mullins & Sekerka (1963) provided a rigorous basis of linear morphological instability at low solidification velocities. Trivedi & Kurz (1986) advanced the analysis of Mullins & Sekerka (1963) for the case of rapid solidification and developed stability criteria dependent upon the interfacial velocity. Following the analytical procedure of Trivedi & Kurz (1986), Galenko & Danilov (2004) extended the model by introducing the local non-equilibrium in the solute diffusion field around the interface. Using this model, they presented a self-consistent analysis of the neutral and absolute morphological stability of a rapidly moving interface. In liquid–solid systems, the most common supplemental constitutive relation to correlate solute concentration to the geometric properties of the interface is the Gibbs–Thomson equation (Volmer 1939).

The goal of this work is to extend the understanding of the Rayleigh–Taylor instability to account for transformation between the two liquid phases. This problem is of natural importance, just as it is for the liquid–vapour and liquid–solid phase transformations. Specifically, the behaviour of a planar interface under one-dimensional infinitesimal sinusoidal disturbances is studied (figure 1). The phases above and below the interface are denoted by (+) and (−), respectively. When a phase transformation occurs across the interface, the interfacial expressions for balance of mass, momentum

https://doi.org/10.1017/S002211200600067X Published online by Cambridge University Press

and energy fail to provide a closed description and must be supplemented by an equation that accounts for the microphysics underlying the exchange of material between the phases. The Hertz–Knudsen–Langmuir and Gibbs–Thomson equations serve this role in sharp-interface models for liquid–vapour and liquid–solid phase transformations, respectively. The Gibbs–Thomson equation is typically derived using a variational argument which rules out the consideration of dissipative mechanisms. Gurtin & Struthers (1990) took a completely different point of view and used an argument based on invariance under observer changes to conclude that a configurational force momentum should join the standard force momentum as a basic law of continuum physics. On this basis, Anderson *et al.* (2006) developed a complete set of equations governing the evolution of a sharp interface separating two fluids undergoing transformation. In this paper, the bulk and interfacial evolution equations considered are the isothermal specialization of equations derived by Anderson *et al.* (2005).

For the bulk phases, the evolution equations are standard and consist of the continuity equation

$$\operatorname{div} \boldsymbol{u} = 0 \tag{1.3}$$

and the linear momentum balance

$$\varrho \frac{\mathrm{D}\boldsymbol{u}}{\mathrm{D}t} = -\operatorname{grad} p_e + \operatorname{div} \boldsymbol{S}, \tag{1.4}$$

where $\varrho = \varrho^{\pm}$ is the constant density in the $(\pm)$ phase, p_e is the effective pressure accounting for the potential of the gravitational body force density $-\varrho \boldsymbol{g}$, and the extra stress in the $(\pm)$ phase is simply

$$\boldsymbol{S} = 2\mu^{\pm} \boldsymbol{D}, \tag{1.5}$$

where $\mu = \mu^{\pm}$ is the (constant) viscosity the $(\pm)$ phase and $\boldsymbol{D} = (\operatorname{grad} \boldsymbol{u} + (\operatorname{grad} \boldsymbol{u})^{\mathsf{T}})/2$ is the rate-of-stretch. By treating the phases as incompressible, we, in effect, model them as large reservoirs with spatially uniform and time-independent densities that are unaffected by mass exchange across the interface. Importantly, the densities of the phases differ.

On the interface, the evolution equations consist of the mass balance, the linear momentum balance, and the normal configurational momentum balance. The interfacial mass balance has the form

$$[\![\varrho(V - \boldsymbol{u} \cdot \boldsymbol{n})]\!] = 0 \qquad \text{or} \qquad J = \varrho^{+}(V - \boldsymbol{u}^{+} \cdot \boldsymbol{n}) = \varrho^{-}(V - \boldsymbol{u}^{-} \cdot \boldsymbol{n}), \tag{1.6}$$

where $[\![\varphi]\!] = \varphi^{+} - \varphi^{-}$ denotes the difference between the interfacial limits of a bulk field in the $(+)$ and $(-)$ phases, $\boldsymbol{n}$ is the interfacial unit normal directed from the $(-)$ phase into the $(+)$ phase, V is the scalar normal velocity of the interface in the direction of $\boldsymbol{n}$, and J is the mass flux normal to the interface. The interfacial linear momentum balance has the form

$$[\![\boldsymbol{S}]\!]\boldsymbol{n} - [\![p_e]\!]\boldsymbol{n} - J^2[\![1/\varrho]\!]\boldsymbol{n} = -\gamma K \boldsymbol{n} - \operatorname{div}_{\mathscr{S}} \mathbb{S}, \tag{1.7}$$

where $\gamma > 0$ is the (constant) interfacial tension, K is the total curvature (i.e. twice the mean curvature) of the interface, and the surface extra stress $\mathbb{S}$ is of the classical form (Boussinesq 1913; Scriven 1960)

$$\mathbb{S} = \lambda(\operatorname{tr} \mathbb{D})\mathbb{P} + 2\alpha \mathbb{D}, \tag{1.8}$$

where $\mathbb{P} = \mathbf{1} - \boldsymbol{n} \otimes \boldsymbol{n}$ is the interfacial projector, $\mathbb{D} = \mathbb{P}\langle\!\langle \boldsymbol{D} \rangle\!\rangle \mathbb{P}$ is the interfacial rate of stretch (with $\langle\!\langle \varphi \rangle\!\rangle = (\varphi^{+} + \varphi^{-})/2$ being the average of the interfacial limits

https://doi.org/10.1017/S002211200600067X Published online by Cambridge University Press

of a bulk field φ in the (+) and (−) phases), and $\lambda + \alpha > 0$ and $\alpha > 0$ and are the (constant) dilatational and shear viscosities of the interface. The normal configurational momentum balance has the form

$$\Psi - \boldsymbol{n} \cdot [\![\boldsymbol{S}/\varrho]\!]\boldsymbol{n} + [\![p_e/\varrho]\!] + \tfrac{1}{2}J^2[\![1/\varrho^2]\!] = \langle\!\langle 1/\varrho \rangle\!\rangle \{\kappa V^{mig} - \beta \Delta_{\mathscr{S}} V^{mig} + \mathbb{S} : \mathbb{K}\}, \quad (1.9)$$

where Ψ is the (constant) specific free energy of the (+) phase relative to that of the (−) phase, $V^{mig} = V - \langle\!\langle \boldsymbol{u} \rangle\!\rangle \cdot \boldsymbol{n}$ is the migrational velocity of the interface, $\Delta_{\mathscr{S}}$ – which is defined for any surface field φ by $\Delta_{\mathscr{S}}\varphi = \mathrm{div}_{\mathscr{S}}(\mathrm{grad}_{\mathscr{S}}\varphi)$ – is the *Laplace–Beltrami* operator on the interface, $\mathbb{K}$ is the curvature tensor of the interface, and $\kappa > 0$ and $\beta > 0$ are the (constant) migrational viscosities of the interface. Whereas κ is associated with viscous drag that impedes the local motion of the interface normal to itself, β is associated with viscous drag that impedes the local reorientation of the interface. For further discussion of these viscosities, see Anderson *et al.* (2005).

As Anderson *et al.* (2005) note, the linear momentum balance (1.7) and the normal configurational momentum balance (1.9) combine to yield the relation

$$\Psi - [\![1/\varrho]\!]\boldsymbol{n} \cdot \langle\!\langle \boldsymbol{S} \rangle\!\rangle \boldsymbol{n} + [\![1/\varrho]\!]\langle\!\langle p_e \rangle\!\rangle = -\langle\!\langle 1/\varrho \rangle\!\rangle \{\gamma K - \kappa V^{mig} + \beta \Delta_{\mathscr{S}} V^{mig}\}, \quad (1.10)$$

which can be imposed in place of (1.9). Simplifying assumptions that reduce (1.10) to the Gibbs–Thomson equation are discussed by Anderson *et al.* (2006).

For a viscous fluid ($\mu^+ \neq 0$ and $\mu^- \neq 0$), the interface conditions (1.6)–(1.9) are supplemented by the kinematical condition

$$\mathbb{P}[\![\boldsymbol{u}]\!] = \boldsymbol{0}, \quad (1.11)$$

which enforces the requirement that the phases do not slip with respect to one another.

The objective of this paper is to investigate the linear instability for an incompressible Newtonian fluid undergoing a liquid–liquid phase transformation. The governing equations are linearized in the standard manner. For inviscid fluids, the interface conditions (1.6)–(1.9) are used to correlate the three disturbace amplitudes arising from the bulk equations (1.3) and (1.4) (with $\boldsymbol{S} = \boldsymbol{0}$). Similarly, when viscosity is taken into account, the supplemental no-slip condition (1.11) for the interface is used in addition to (1.6)–(1.9) to determine the five unknown disturbance amplitudes arising from the bulk equations (1.3) and (1.4). For inviscid fluids, we consider the influence of the initial mass flux across the interface on the growth of the disturbance. This effect is found to stabilize the disturbed system by moderating the propagation of the growth rate and decreasing the range of unstable wavenumbers. For viscous fluids, we consider only the case where the base state does not involve mass transfer between the phases. In this case, the cutoff wavenumber is found to be identical to that of the classical Rayleigh–Taylor problem. Moreover, the disturbances are found to grow significantly faster than those of the classical Rayleigh–Taylor problem. The effects of the Reynolds number, Weber number, and Froude number on the growth rate of the disturbance are all considered. Also, the presence of the various interfacial viscosities α, $\alpha+\lambda$, κ and β leads to the consideration of three additional dimensionless quantities – the Boussinesq, Voronkov, and Gurtin numbers – all of which attenuate the growth of disturbances.

2. Base state

Using notation consistent with figure 1, consider a stationary base state in which the (−) and (+) phases occupy the time-dependent regions $\{\boldsymbol{x} : x_2 < V_0 t\}$ and $\{\boldsymbol{x} : x_2 > V_0 t\}$, repectively. The interface then corresponds to the time-dependent

https://doi.org/10.1017/S002211200600067X Published online by Cambridge University Press

surface $\{\boldsymbol{x} : x_2 = V_0 t\}$. Suppose that the velocity and pressure in the base state are constant and given by $\boldsymbol{u}_0^{\pm} = u_0 \mathbf{e}_1 + v_0^{\pm} \mathbf{e}_2$ and $p_0^{\pm}$. The bulk equations (1.3) and (1.4) then hold trivially. However, the interfacial equations (1.6), (1.7) and (1.9) require that the parameters $v_0^{\pm}$, $p_0^{\pm}$ and V_0 describing the base state be consistent with the equations

$$[\![\varrho(V_0 - v_0)]\!] = 0, \tag{2.1a}$$

$$[\![p_e]\!] + J_0^2 [\![1/\varrho]\!] = 0, \tag{2.1b}$$

$$\Psi + [\![p_e/\varrho]\!] + \tfrac{1}{2} J_0^2 [\![1/\varrho^2]\!] = \langle\!\langle 1/\varrho \rangle\!\rangle \kappa (V_0 - \langle\!\langle v_0 \rangle\!\rangle), \tag{2.1c}$$

where

$$J_0 = \varrho^+(V_0 - v_0^+) = \varrho^-(V_0 - v_0^-) \tag{2.2}$$

denotes the mass flux across the interface in the base state.

When $J_0 = 0$, there is no mass transport between the phases in the base state. By (2.2),

$$v_0^+ = v_0^- = V_0 \tag{2.3}$$

and the fluid velocity is continuous in the base state. Moreover, (2.1*b*) and (2.1*c*) reduce to

$$[\![p_e]\!] = 0, \qquad \Psi + [\![p_e/\varrho]\!] = 0. \tag{2.4}$$

3. Inviscid case

We first consider the idealized case of a fluid that is inviscid in the sense that the bulk viscosities μ^+ and μ^- as well as the interfacial viscosities α, λ, κ and β vanish. For such a fluid, the linear momentum balance (1.4) becomes

$$\varrho \frac{\mathrm{D}\boldsymbol{u}}{\mathrm{D}t} = -\operatorname{grad} p_e. \tag{3.1}$$

Further, the interfacial linear momentum balance (1.7) and the normal configurational momentum balance (1.9) become

$$[\![p_e]\!] + J^2 [\![1/\varrho]\!] = \gamma K, \tag{3.2a}$$

$$\Psi + [\![p_e/\varrho]\!] + \tfrac{1}{2} J^2 [\![1/\varrho^2]\!] = 0. \tag{3.2b}$$

3.1. *Bulk disturbance*

For an infinitesimal sinusoidal increment, indicated by the subscript 1, to the base state, the velocity and pressure in the $(\pm)$ phase become $\boldsymbol{u}^{\pm} = \boldsymbol{u}_0^{\pm} + \epsilon \boldsymbol{u}_1^{\pm}$ and $p^{\pm} = p_0^{\pm} + \epsilon p_1^{\pm}$, with $\epsilon \ll 1$ and

$$(u_1^{\pm}, v_1^{\pm}, p_1^{\pm})(x_1, x_2, t) = (u_1^{\pm}, v_1^{\pm}, p_1^{\pm})(y) \exp\left\{ \mathrm{i}kx + \frac{\omega t}{|At|T} \right\}, \tag{3.3}$$

where

$$x = \frac{x_1 - u_0 t}{L}, \qquad y = \frac{x_2 - V_0 t}{L}, \tag{3.4a, b}$$

$k > 0$ is the dimensionless wavenumber of the perturbation, ω is the dimensionless growth rate of the perturbation, and L and T are characteristic length and time scales.

Inserting (3.3) into the continuity equation (1.3) and the momentum balance (3.1), neglecting terms of $O(\epsilon^2)$, and cancelling a common factor of $\exp(\mathrm{i}kx + \omega t/|At|T)$ from each term, we arrive at a system of three ordinary differential equations for each

https://doi.org/10.1017/S002211200600067X Published online by Cambridge University Press

phase. On writing $\mathrm{D} = \mathrm{d}/\mathrm{d}y$, that system takes the form

$$\mathrm{i}ku_1^{\pm} + \mathrm{D}v_1^{\pm} = 0, \tag{3.5a}$$

$$\varrho^{\pm}\left\{\frac{V_0 - v_0^{\pm}}{L}\mathrm{D} - \frac{\omega}{|At|T}\right\}u_1^{\pm} = \frac{\mathrm{i}k}{L}p_1^{\pm}, \tag{3.5b}$$

$$\varrho^{\pm}\left\{\frac{V_0 - v_0^{\pm}}{L}\mathrm{D} - \frac{\omega}{|At|T}\right\}v_1^{\pm} = \frac{1}{L}\mathrm{D}p_1^{\pm}. \tag{3.5c}$$

Eliminating $p_1^{\pm}$ and $u_1^{\pm}$ from this system yields an ordinary differential equation,

$$(\mathrm{D}^2 - k^2)\left\{J_0\mathrm{D} - \frac{\varrho^{\pm}L\omega}{|At|T}\right\}v_1^{\pm} = 0, \tag{3.6}$$

for $v_1^{\pm}$. The characteristic roots of this equation are $\pm k$ and, when $J_0 \neq 0$, $\varrho^{\pm}L\omega/J_0|At|T$. To rule out infinite fluid velocities in the far field, we exclude from consideration the last of these roots (which is of indeterminate sign) and take v_1 to be of the form

$$v_1(y) = \begin{cases} A^+\exp(-ky), & y > 0, \\ A^-\exp(ky), & y < 0, \end{cases} \tag{3.7}$$

with A^+ and A^- being unknown amplitudes. In view of (3.7), the system (3.5) yields expressions

$$u_1(y) = \begin{cases} -\mathrm{i}A^+\exp(-ky), & y > 0, \\ \mathrm{i}A^-\exp(ky), & y < 0, \end{cases} \tag{3.8}$$

and

$$p_1(y) = \begin{cases} A^+\left\{J_0 + \dfrac{\varrho^+L\omega}{|At|Tk}\right\}\exp(-ky), & y > 0, \\ A^-\left\{J_0 - \dfrac{\varrho^-L\omega}{|At|Tk}\right\}\exp(ky), & y < 0, \end{cases} \tag{3.9}$$

for u_1 and p_1.

3.2. *Interfacial disturbance*

We assume that the bulk disturbance is accompanied by an infinitesimal interfacial disturbance of the form $x_2 = V_0t + \epsilon F(x_1, t)$. Direct calculations then show that

$$\left.\begin{gathered} \boldsymbol{n} \sim -\epsilon\frac{\partial F}{\partial x_1}\boldsymbol{e}_1 + \boldsymbol{e}_2, \qquad K \sim \epsilon\frac{\partial^2 F}{\partial x_1^2}, \\ V \sim V_0 + \epsilon\frac{\partial F}{\partial t}, \qquad J \sim J_0 + \epsilon\varrho^{\pm}\left\{\frac{\partial F}{\partial t} + u_0\frac{\partial F}{\partial x_1} - v_1^{\pm}\right\}, \\ V^{mig} \sim V_0^{mig} + \epsilon\left\{\frac{\partial F}{\partial t} + u_0\frac{\partial F}{\partial x_1} - \langle\!\langle v_1\rangle\!\rangle\right\}. \end{gathered}\right\} \tag{3.10}$$

Consistent with the form (3.3) of the bulk disturbance, we take

$$F(x_1, t) = C\exp\left\{\mathrm{i}kx + \frac{\omega t}{|At|T}\right\}, \tag{3.11}$$

where x is as defined in (3.4*a*) and C is an additional unknown amplitude.

https://doi.org/10.1017/S002211200600067X Published online by Cambridge University Press

3.3. *Amplitude equations*

The bulk and interfacial disturbances involve three unknown amplitudes A^+, A^- and C. However, we have yet to make use of the interface conditions (1.6), (3.2*a*) and (3.2*b*) expressing mass balance, linear momentum balance and normal configurational momentum balance. Inserting the assumed forms for the velocity and the interface profile in the mass balance (1.6), using (3.7) and (3.8), and invoking the condition (2.1*a*) in the base state, dropping terms of $O(\epsilon^2)$, and cancelling a common factor of $\exp(ikx + \omega t/|At|T)$ from each term, we obtain

$$\varrho^+ A^+ - \varrho^- A^- = \frac{2\langle\!\langle \varrho \rangle\!\rangle \omega}{T} C. \tag{3.12}$$

Proceeding similarly with the linear momentum balance (3.2*a*) and the normal configurational momentum balance (3.2*b*), we obtain

$$\varrho^+ \left\{ \frac{J_0 k}{\varrho^-} + \frac{L\omega}{|At|T} \right\} A^+ - \varrho^- \left\{ \frac{J_0 k}{\varrho^+} - \frac{L\omega}{|At|T} \right\} A^- = \left\{ [\![\varrho]\!] g - \frac{\gamma k^2}{L^2} + \frac{2J_0 \langle\!\langle \varrho \rangle\!\rangle [\![\varrho]\!] \omega}{\varrho^+ \varrho^- |At|T} \right\} kC, \tag{3.13}$$

where $g = |\boldsymbol{g}|$ denotes the magnitude of the acceleration due to gravity, and

$$\left\{ \varrho^+ J_0 \langle\!\langle 1/\varrho^2 \rangle\!\rangle k + \frac{L\omega}{|At|T} \right\} A^+ - \left\{ \varrho^- J_0 \langle\!\langle 1/\varrho^2 \rangle\!\rangle k - \frac{L\omega}{|At|T} \right\} A^- = \frac{2\langle\!\langle \varrho \rangle\!\rangle^2 [\![\varrho]\!] k\omega}{(\varrho^+ \varrho^-)^2 |At|T} C. \tag{3.14}$$

3.4. *Dispersion relation*

Equations (3.12)–(3.14) provide a homogeneous linear system for the disturbance amplitudes A^+, A^- and C. Had we imposed only mass balance and linear momentum balance on the interface, this system would be underdetermined. This underlines the need for an additional interface condition – provided here by the normal configurational momentum balance – to account for the microphysics of the phase transformation. Necessary and sufficient for the system (3.12)–(3.14) to yield a non-trivial solution is the requirement that its determinant vanish. This requirement yields the dispersion relation

$$\omega^2 + \left\{ \frac{\gamma k^2}{2\langle\!\langle \varrho \rangle\!\rangle g L^2} - At \right\} \frac{gT^2 k}{L} + \frac{J_0^2 T^2 At^2 k^2}{\varrho^+ \varrho^- L^2} = 0. \tag{3.15}$$

Defining the Weber and Froude numbers via

$$We = \frac{\langle\!\langle \varrho \rangle\!\rangle g L^2}{\gamma}, \qquad Fr = \frac{L}{gT^2}, \tag{3.16}$$

and introducing the dimensionless interfacial mass flux

$$J = \frac{J_0 T}{\langle\!\langle \varrho \rangle\!\rangle L}, \tag{3.17}$$

we may rewrite the dispersion relation (3.15) in the form

$$\omega^2 = \left\{ At - \frac{k^2}{2We} \right\} \frac{k}{Fr} - \frac{At^2 J^2 k^2}{1 - At^2}. \tag{3.18}$$

https://doi.org/10.1017/S002211200600067X Published online by Cambridge University Press

3.5. *Analysis of the dispersion relation*

3.5.1. *Base process without mass transport:* $\jmath = 0$

We consider first the case where the base state does not involve mass transport across the interface, so that $\jmath = 0$ and (3.18) reduces to

$$\omega^2 = \left\{ At - \frac{k^2}{2We} \right\} \frac{k}{Fr}. \tag{3.19}$$

From (3.19), it follows immediately that the base state is linearly unstable when $At > 0$ and the wavenumber k obeys $0 < k < k_c = \sqrt{2At\,We} = \sqrt{[\![\varrho]\!] g/\gamma}\, L$. Bearing in mind that k is dimensionless, the cutoff wavenumber is equivalent to that derived by Bellman & Pennington (1954) for the classical Rayleigh–Taylor problem. When $At < 0$, so that the phase with the lower density is above that with the higher density, the growth rate ω is pure imaginary and the system is neutrally stable. Hence, for an inviscid fluid and a base state with $\jmath = 0$, the stability results are the same as those for the classical Rayleigh–Taylor problem.

3.5.2. *Base process with mass transport:* $\jmath \neq 0$

When $\jmath \neq 0$, (3.18) includes a stabilizing term associated with the exchange of mass between the phases in the base state. This term influences both the range of unstable wavenumbers and the magnitude of the growth rate when instability is present. In particular, an easy calculation shows that when $\jmath \neq 0$, the cutoff wavenumber k_c below which perturbations are unstable is given by

$$k_c = \sqrt{\left(\frac{We\,Fr\,At^2\jmath^2}{1 - At^2} \right)^2 + 2At\,We} - \frac{We\,Fr\,At^2\jmath^2}{1 - At^2}. \tag{3.20}$$

Since $\sqrt{a^2 + b} \leqslant a + \sqrt{b}$ for $a > 0$ and $b > 0$, it follows that k_c as given by (3.20) is less than or equal to the cutoff wavenumber $\sqrt{2At\,We}$ for classical Rayleigh–Taylor problem. Further, when $\jmath \neq 0$, the maximum growth rate ω_m is given by

$$\omega_m = \sqrt{\left(At - \frac{k_m^2}{2We} \right) \frac{k_m}{Fr} - \frac{At^2\jmath^2k_m^2}{1 - At^2}}, \tag{3.21}$$

where k_m, which is the most unstable wavenumber, is defined by

$$k_m = \frac{2}{3} \left\{ \sqrt{\left(\frac{We\,Fr\,At^2\jmath^2}{1 - At^2} \right)^2 + \frac{3At\,We}{2}} - \frac{We\,Fr\,At^2\jmath^2}{1 - At^2} \right\}. \tag{3.22}$$

Careful examination of (3.20) and (3.21) reveals that neither k_c nor ω_m grows monotonically with the Atwood number At: k_c and ω_m both vanish for the limit $At \to 0$, attain maxima at disparate values of At in the open interval (0, 1), and vanish for the limit $At \to 1$. This behaviour is illustrated in figure 2 for $We = 0.1$ and $Fr = 1$.

Again, since $\sqrt{a^2 + b} \leqslant a + \sqrt{b}$ for $a > 0$ and $b > 0$, it follows from (3.22) that

$$k_m \leqslant \sqrt{\frac{2At\,We}{3}}. \tag{3.23}$$

Hence, the most unstable wavenumber for the problem involving a phase transformation is always less than or equal to its counterpart for the classical Rayleigh–Taylor problem. This behaviour is illustrated in figure 3 for $We = 0.1$ and $Fr = 1$.

https://doi.org/10.1017/S002211200600067X Published online by Cambridge University Press

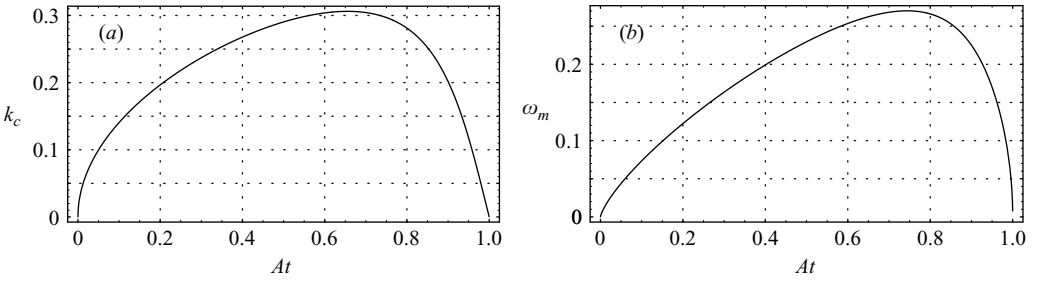


FIGURE 2. Variation of the cutoff wavenumber k_c and the maximum growth rate ω_m with the Atwood number At: (*a*) k_c; (*b*) ω_m. Combinations of k and At below the k_c-curve are unstable. $We = 0.1$; $Fr = 1$; $J = 0.9$.

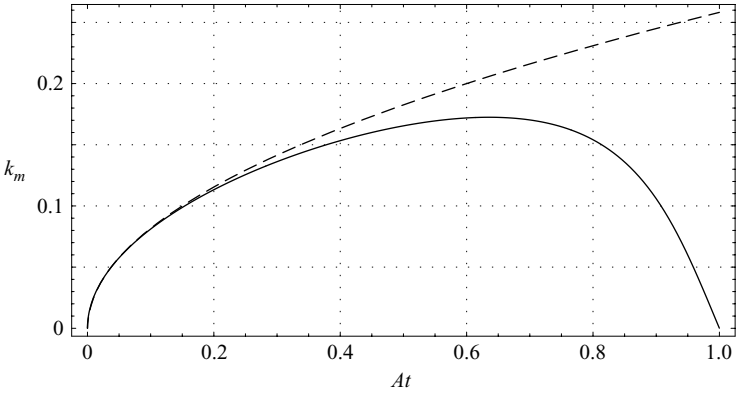


FIGURE 3. Variation of the most unstable wavenumber k_m with the Atwood number At. Solid line: phase transformation. Dashed line: no phase transformation. $We = 0.1$; $Fr = 1$.

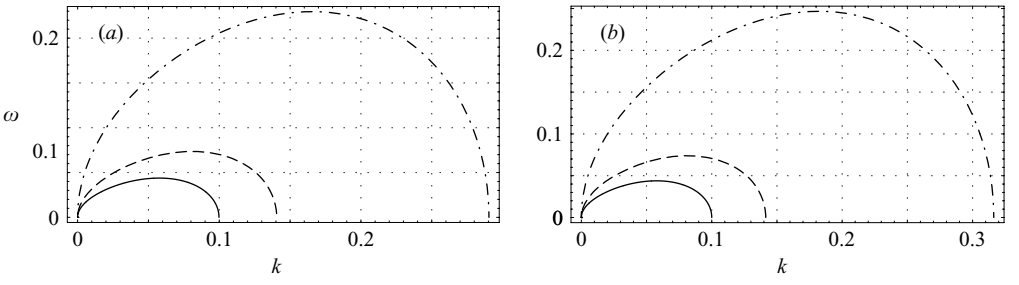


FIGURE 4. Comparison of the relation for the growth rate ω versus the wavenumber k for various values of the Atwood number At: (*a*) $J = 0.9$ (*b*) no phase transformation. $We = 0.1$; $Fr = 1$. —, $At = 0.05$; - - -, 0.1; –·–, 0.5.

Plots of the growth rate ω versus the wavenumber k for the Rayleigh–Taylor problem with a phase transformation (with $J = 0.9$) and the classical Rayleigh–Taylor problem are provided, for $We = 0.1$, $Fr = 1$, and various values of At, in figure 4. Consistent with the foregoing discussion, these plots show little difference when $At \ll 1$. However, for relatively large At, the growth rate of any unstable mode is considerably depressed and the cutoff wavenumber below which perturbations are unstable is reduced.

https://doi.org/10.1017/S002211200600067X Published online by Cambridge University Press

Referring to (3.18), we observe that the growth rate increases with increasing Weber number *We*, but decreases with increasing Froude number *Fr*.

Even when interfacial tension is neglected, the mass transport term stabilizes the system when the disturbance wave number is above the cutoff wavenumber $k_c = (1 - At^2)/At\,Fr\,\jmath^2$. This stabilizing effect also vanishes when $At \to 1$.

Finally, although intuitive reasoning might suggest that, of the two possibilities, only a mass flux from the (−) phase to the (+) phase would stabilize the system, our linear analysis indicates that the direction of the mass flow in the base state does not affect stability since the dimensionless mass flux coefficient $\jmath$ appears in (3.18) only in terms of $\jmath^2$. A linear analysis carried to a higher order or a nonlinear analysis might lead to different conclusions regarding the role of the direction of mass flow in the base state. The inclusion of viscosity is also likely to alter the stability of the system.

4. Viscous case

We now study the influence of the various viscosities on the stability of the base state. For simplicity, we take the kinematic viscosities of the phases to be equal, so that

$$\frac{\mu^+}{\varrho^+} = \frac{\mu^-}{\varrho^-} = \nu. \tag{4.1}$$

As an additional simplifying assumption, we confine attention to base states that do not involve mass exchange between the phases. (Mass exchange in response to the perturbation of the interface is, however, allowed.) Thus, $J_0 = 0$ and $v_0^+ = v_0^- = V_0$.

We consider bulk and interfacial disturbances identical to those imposed in the inviscid case. Proceeding as in the inviscid case, the continuity equation (1.3) and the momentum balance (1.4) yield (3.5*a*) and

$$\left.\begin{aligned} \varrho^{\pm}\left\{\frac{\nu}{L^2}(\mathrm{D}^2 - k^2) - \frac{\omega}{|At|T}\right\}u_1^{\pm} &= \frac{\mathrm{i}k}{L}p_1^{\pm}, \\ \varrho^{\pm}\left\{\frac{\nu}{L^2}(\mathrm{D}^2 - k^2) - \frac{\omega}{|At|T}\right\}v_1^{\pm} &= \frac{1}{L}\mathrm{D}p_1^{\pm}. \end{aligned}\right\} \tag{4.2}$$

Eliminating $p_1^{\pm}$ and $u_1^{\pm}$ from this system yields an ordinary differential equation,

$$(\mathrm{D}^2 - k^2)(\mathrm{D}^2 - q^2)v_1^{\pm} = 0 \qquad \text{with} \qquad q = \sqrt{k^2 + \frac{L^2\omega}{|At|T\nu}}, \tag{4.3}$$

for $v_1^{\pm}$. To rule out infinite fluid velocities in the far field, we choose v_1 to be of the form

$$v_1(y) = \begin{cases} A^+\exp(-ky) + B^+\exp(-qy), & y > 0, \\ A^-\exp(ky) + B^-\exp(qy), & y < 0, \end{cases} \tag{4.4}$$

where $A^{\pm}$ and $B^{\pm}$ are unknown amplitudes. In view of (4.4), (3.5*a*) and (4.2) yield expressions

$$u_1(y) = \begin{cases} -\mathrm{i}A^+\exp(-ky) - \dfrac{\mathrm{i}B^+q}{k}\exp(-qy), & y > 0, \\ \mathrm{i}A^-\exp(ky) + \dfrac{\mathrm{i}B^-q}{k}\exp(qy), & y < 0, \end{cases} \tag{4.5}$$

https://doi.org/10.1017/S002211200600067X Published online by Cambridge University Press

and

$$p_1(y) = \begin{cases} \dfrac{A^+\varrho^+ L\omega}{|At|Tk}\exp(-ky), & y > 0, \\ -\dfrac{A^-\varrho^- L\omega}{|At|Tk}\exp(ky), & y < 0, \end{cases} \tag{4.6}$$

for u_1 and p_1.

When viscosity is taken into account, the interface conditions (1.6), (1.7) and (1.9) imposing mass balance, linear momentum balance and configurational momentum balance supplemented by the no-slip condition (1.11) lead to a system of five equations connecting the unknown amplitudes A^+, A^-, B^+, B^- and C of the disturbance. Proceeding as in the inviscid case, but making use of the simplified base equations (2.4) instead of (2.1*b*) and (2.1*c*), we find that the mass balance (1.6) yields

$$\varrho^+(A^+ + B^+) - \varrho^-(A^- + B^-) = \frac{[\![\varrho]\!]\omega}{|At|T}C. \tag{4.7}$$

In contrast to the inviscid case, the linear momentum balance (1.7) now gives rise to non-trivial components in both the $\mathbf{e}_1$ and the $\mathbf{e}_2$ directions. In the $\mathbf{e}_1$-direction, (1.7) yields

$$\begin{aligned} &\left\{2\varrho^+k^2 + \frac{(\alpha+\frac{1}{2}\lambda)k^3}{\nu L}\right\}A^+ + \left\{\varrho^+(k^2+q^2) + \frac{(\alpha+\frac{1}{2}\lambda)k^2q}{\nu L}\right\}B^+ \\ &\quad - \left\{2\varrho^-k^2 + \frac{(\alpha+\frac{1}{2}\lambda)k^3}{\nu L}\right\}A^- - \left\{\varrho^-(k^2+q^2) + \frac{(\alpha+\frac{1}{2}\lambda)k^2q}{\nu L}\right\}B^- = 0. \end{aligned} \tag{4.8}$$

Importantly, (4.8) involves the combination $\alpha + \lambda/2$ of α and λ. Since $\alpha > 0$ and $\alpha + \lambda > 0$, it follows that $\alpha + \lambda/2 = \alpha/2 + (\alpha + \lambda)/2 > 0$. Hereinafter, we refer to $\alpha + \lambda/2$ as the effective viscosity of the interface. Further, in the $\mathbf{e}_2$-direction, (1.7) yields

$$\left\{\frac{2\nu k^2}{L^2} + \frac{\omega}{|At|T}\right\}(\varrho^+A^+ + \varrho^-A^-) + \frac{2\nu kq}{L^2}(\varrho^+B^+ + \varrho^-B^-) = \frac{k}{L}\left\{[\![\varrho]\!]g - \frac{\gamma k^2}{L^2}\right\}C. \tag{4.9}$$

Next, the normal configurational momentum balance yields (1.9)

$$\begin{aligned} &\left\{\frac{2\nu k^2}{L^2} + \left(\kappa + \frac{\beta k^2}{L^2}\right)\frac{\langle\!\langle 1/\varrho\rangle\!\rangle k}{2L} + \frac{\omega}{|At|T}\right\}(A^+ + A^-) \\ &+ \left\{\frac{2\nu kq}{L^2} + \left(\kappa + \frac{\beta k^2}{L^2}\right)\frac{\langle\!\langle 1/\varrho\rangle\!\rangle k}{2L}\right\}(B^+ + B^-) = \left\{\kappa + \frac{\beta k^2}{L^2}\right\}\frac{\langle\!\langle 1/\varrho\rangle\!\rangle k\omega}{|At|LT}C. \end{aligned} \tag{4.10}$$

Finally, the no-slip condition (1.11) yields

$$kA^+ + qB^+ + kA^- + qB^- = 0. \tag{4.11}$$

The dispersion relation arising from the requirement that the determinant of the homogeneous system (4.7)–(4.11) vanish takes the form

$$\begin{aligned} &\frac{2\omega^2 q}{|At|}\left\{\omega^2 + \frac{4|At|k^2\omega}{Re} - \frac{4At^2k^3(q-k)}{Re^2} + \left(\frac{k^2}{2We} - At\right)\frac{k}{Fr}\right\} \\ &\quad + \frac{2Bok^2q\omega}{Re}\left\{q\omega^2 + \left(\frac{k^2}{2We} - At\right)\frac{k(q-k)}{Fr}\right\} - k\omega\left\{\frac{1}{Vo} + \frac{k^2}{Gu}\right\}\left\{\left(k - \frac{q}{At^2}\right)\omega^2\right. \end{aligned}$$

https://doi.org/10.1017/S002211200600067X Published online by Cambridge University Press

$$-k(q-k)\left(\frac{4|At|k}{Re}\left(\omega-\frac{|At|k(q-k)}{Re}\right)+\frac{k^2}{2WeFr}-\frac{At}{Fr}\right)\Bigg\}+\frac{Bok^3(q-k)}{Re}$$
$$\times\left\{\frac{1}{Vo}+\frac{k^2}{Gu}\right\}\left\{\frac{2q\omega^2}{|At|}+\left(\frac{k^2}{2We}-At\right)\frac{|At|k(q-k)}{Fr}\right\}=0, \quad (4.12)$$

where

$$Re=\frac{L^2}{\nu T}, \quad Bo=\frac{\lambda+2\alpha}{2\langle\!\langle\varrho\rangle\!\rangle\nu L}, \quad Vo=\frac{L}{\langle\!\langle 1/\varrho\rangle\!\rangle\kappa T}, \quad \text{and} \quad Gu=\frac{L^3}{\langle\!\langle 1/\varrho\rangle\!\rangle\beta T} \quad (4.13)$$

are the Reynolds number, the Boussinesq number, the Voronkov number and the Gurtin number. To the best of our knowledge, the migrational viscosity κ was first introduced by Voronkov (1964) in his extension of the Gibbs–Thomson relation to account for interfacial attachment kinetics. We therefore refer to the associated dimensionless number as the Voronkov number. The migrational viscosity β, associated with the change of orientation of the interface, was first introduced by Anderson *et al.* (2005). We therefore refer to the associated dimensionless number as the Gurtin number.

We next explore the influence of the dimensionless parameters *Re*, *Bo*, *Vo* and *Gu* associated with the viscosity of the liquid phases and the effective and migrational viscosities of the interface on the stability of the base process. As in the inviscid case, we find it useful to make comparisons with results from the classical Rayleigh–Taylor problem. For this problem the normal configurational momentum balance is irrelevant and is replaced by the requirement $V^{mig}=0$ that the interface be material. When combined, the mass balance (1.6) and the condition $V^{mig}=0$ yield two interface conditions, $V=\boldsymbol{u}^+\cdot\boldsymbol{n}$ and $V=\boldsymbol{u}^-\cdot\boldsymbol{n}$ to be imposed along with linear momentum balance (1.7) and the no-slip condition (1.11). Granted that the kinematical viscosities of the two fluids are identical, the relevant amplitude equations lead to the dispersion relation

$$\frac{\omega}{|At|}\left\{\left(1+\frac{(1-At^2)q}{At^2(q-k)}\right)\omega^2+\frac{4|At|k^2\omega}{Re}-\frac{4At^2k^3(q-k)}{Re^2}+\left(\frac{k^2}{2We}-At\right)\frac{k}{Fr}\right\}$$
$$+\frac{Bok^2}{Re}\left\{q\omega^2+\left(\frac{k^2}{2We}-At\right)\frac{At^2k(q-k)}{Fr}\right\}=0. \quad (4.14)$$

4.1. *Influence of the kinematical viscosity*

We now consider the influence of kinematical viscosity ν of the phases while neglecting the influences of the effective viscosity $\alpha+\lambda/2$ and migrational viscosities κ and β of the interface. In this case, $Bo=0$, $Vo\to\infty$, $Gu\to\infty$ and the general dispersion relation (4.12) simplifies to

$$\omega^2+\frac{4|At|k^2\omega}{Re}-\frac{4At^2k^3(q-k)}{Re^2}+\left\{\frac{k^2}{2We}-At\right\}\frac{k}{Fr}=0. \quad (4.15)$$

As one might expect, for *At* finite, setting $Re\to\infty$ in (4.15) reduces (4.15) to the dispersion relation (3.19) obtained in the case of an inviscid fluid without mass transport in the base state. Another point of comparison is provided by the appropriate dispersion relation for the classical Rayleigh–Taylor problem. Specifically, when $Bo=0$, (4.14) reduces to (Chandrasekhar 1961)

$$\left\{1+\frac{(1-At^2)q}{At^2(q-k)}\right\}\omega^2+\frac{4|At|k^2\omega}{Re}-\frac{4At^2k^3(q-k)}{Re^2}+\left\{\frac{k^2}{2We}-At\right\}\frac{k}{Fr}=0, \quad (4.16)$$

https://doi.org/10.1017/S002211200600067X Published online by Cambridge University Press

which differs from (4.15) only in the coefficient of ω^2. In particular, upon setting $\omega = 0$ in (4.15) and (4.16), we obtain an equivalent cutoff wavenumber $k_c = \sqrt{2AtWe}$ below which perturbations are unstable. Hence, when the kinematic viscosities of the bulk phases are identical, mass transport is not present in the base state, and the effective and migrational viscosities of the interface, the range of unstable wave numbers for the Rayleigh–Taylor problem with a phase transformation is identical to the range of unstable wavenumbers for the appropriate version of the classical Rayleigh–Taylor problem.

For $At < 0$, it is known that the system is stable for the classical Rayleigh–Taylor problem. We now show that this result also holds when a phase transformation occurs. Assume $At < 0$ and $\omega > 0$. The final term on the left-hand side of (4.15) must therefore be positive and the inequality

$$\omega^2 + \frac{4|At|k^2\omega}{Re} < \frac{4At^2k^3(q-k)}{Re^2} \tag{4.17}$$

must hold. Next, since

$$q = \sqrt{k^2 + \frac{Re\,\omega}{|At|}} = k\sqrt{1 + \frac{Re\,\omega}{|At|k^2}} < k\left\{1 + \frac{Re\,\omega}{2|At|k^2}\right\},$$

it follows from (4.17) that

$$\omega^2 + \frac{4|At|k^2\omega}{Re} < \frac{4At^2k^3(q-k)}{Re^2} < \frac{4At^2k^4}{Re^2}\frac{\omega Re}{2|At|k^2} = \frac{2|At|k^2\omega}{Re}$$

and, thus, that

$$\omega < -\frac{2|At|k^2}{Re} < 0.$$

This last inequality contradicts the assumption that ω be positive. Provided that $At < 0$, we therefore conclude that ω must be negative as well. (For $At < 0$ and ω complex with positive real part, an analogous, but algebraically more involved, argument also leads to a contradication.) Hence, when the kinematical viscosities of the bulk phases are identical, mass transport is not present in the base state, and the effective and migrational viscosities of the interface, instability is possible for the Rayleigh–Taylor problem with a phase transformation only when the phase with the higher density is above that with the lower density.

In view of the foregoing result, we observe that, when $0 < At < 1$, the coefficient of ω^2 in (4.16) is greater than that in (4.15). For equal values of the parameters $0 < At < 1$, Re and Fr, the magnitude of any unstable growth rate obtained from the dispersion relation (4.15) for the problem with a phase transformation will exceed that obtained from the dispersion relation (4.16) for the classical problem.

The parameters Re, We and Fr enter the dispersion relations (4.15) and (4.16) in an identical fashion. The influence of these parameters on stability should not differ for the problems with and without a phase transformation. Specifically, differentiating (4.15) with respect to Fr, we find that for $0 < k < \sqrt{2AtWe}$,

$$2\left\{\omega + \frac{|At|k^2(2q-k)}{Re\,q}\right\}\frac{\partial\omega}{\partial Fr} = \left\{\frac{k^2}{2We} - At\right\}\frac{k}{Fr^2} < 0.$$

Hence, the magnitude of the growth rate of the unstable wave modes decreases with increasing Fr. Similarly, differentiating (4.15) with respect to Re and We, we

https://doi.org/10.1017/S002211200600067X Published online by Cambridge University Press

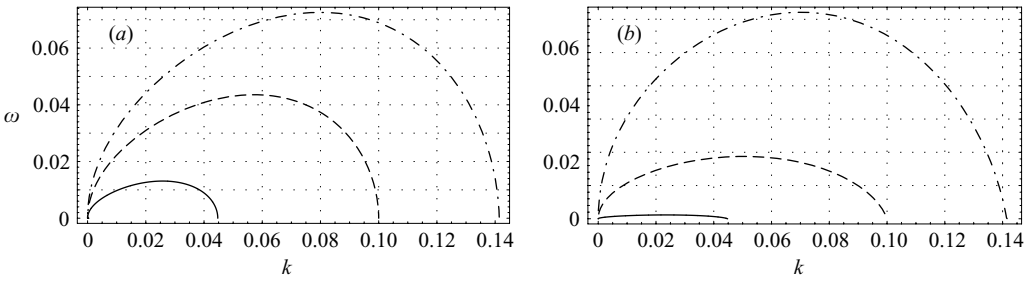


FIGURE 5. Comparison of the relation for the growth rate ω versus the wavenumber k for different Atwood numbers At: (*a*) phase transformation; (*b*) no phase transformation. $Re = 1$; $We = 0.1$; $Fr = 1$; —, $At = 0.01$; – – –, 0.05; –·–, 0.1.

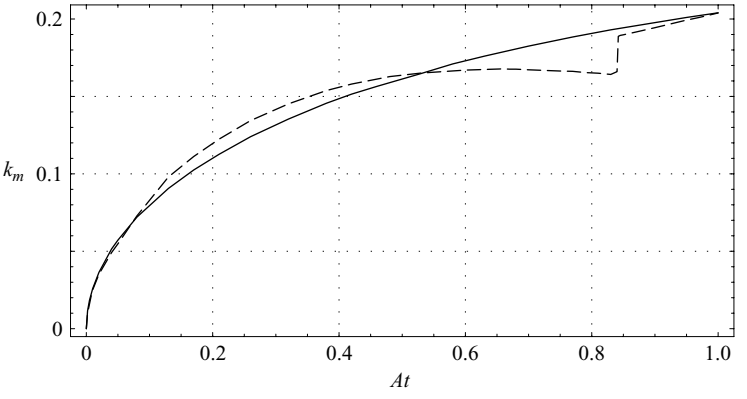


FIGURE 6. Variation of the most unstable wavenumber k_m with the Atwood number At. —, phase transformation; - - -, no phase transformation. $Re = 1$; $We = 0.1$; $Fr = 1$.

find $\partial\omega/\partial Re > 0$ and $\partial\omega/\partial We > 0$ for $0 < k < \sqrt{2AtWe}$. The growth of an unstable perturbation therefore increases for increasing Re and We.

Plots of the growth rate ω versus the wavenumber k for $Re = 1$, $We = 0.1$, $Fr = 1$ and various values of At are provided in figure 5. Consistent with analytical predictions, the cutoff wavenumbers are indistinguishible and the growth rates for a phase interface are at least an order of magnitude greater than those for a material interface. Also, above the cutoff wavenumber, the growth rates for the phase transformation and classical problems are pure imaginary and the base state is neutrally stable.

In constrast to the inviscid case, when the kinematic viscosity of the phases is taken into consideration the most unstable wavenumber k_{m} for the problem with a phase transformation is not necessarily less than or equal to its counterpart for the classical Rayleigh–Taylor problem. This behaviour is illustrated in figure 6, which shows a plot of k_m as a function of At for $Re = 1$, $We = 0.1$, and $Fr = 1$. The behaviour is complicated. Two solution branches exist for the classical problem. We plot only the combination of those branches corresponding to the maximum value of the growth rate. The plot shows that k_m lies below its classical counterpart for At sufficiently close to 0 and 1; however, for intermediate values of At, k_m lies above its classical counterpart.

The effect of varying the Froude number on the stability of the base state is illustrated in figure 7, which shows plots of the growth rate ω versus the wavenumber

https://doi.org/10.1017/S002211200600067X Published online by Cambridge University Press

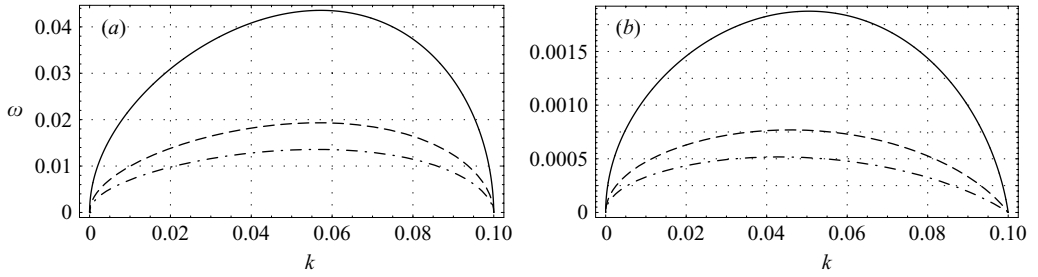


FIGURE 7. Comparison of the relation for the growth rate ω versus the wavenumber k for different Froude numbers Fr: (a) phase transformation; (b) no phase transformation. $At = 0.05$; $Re = 1$; $We = 0.1$; —, $Fr = 1$; - - -, 5; –·–, 10.

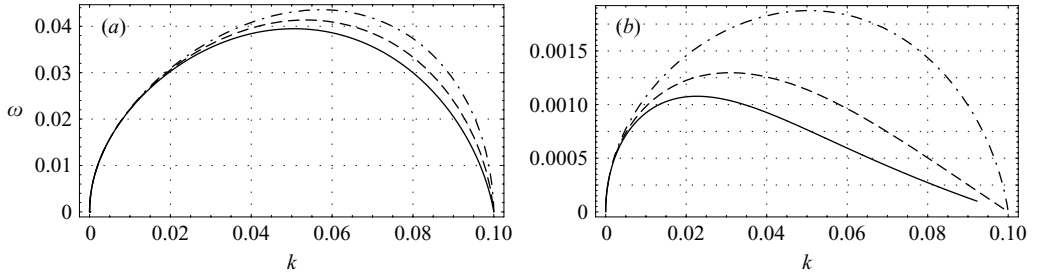


FIGURE 8. Comparison of the relation for the growth rate ω versus the wavenumber k for different Reynolds numbers Re: (a) phase transformation; (b) no phase transformation. $At = 0.05$; $We = 0.1$; $Fr = 1$; —, $Re = 0.05$; - - -, 0.1; –·–, 1.

k for $At = 0.05$, $Re = 1$, $We = 0.1$, and various values of Fr. Consistent with analytical expectations, these plots show that the maximum growth rate decreases with increasing Fr whether or not a phase transformation occurs. Moreover, varying Fr does not affect the range of unstable wavenumbers.

The impact of varying the Reynolds number is more complicated. For $At = 0.5$, $We = 0.1$, and $Fr = 1$, figure 8 shows that, for $Re \leqslant 1$, the system becomes more unstable as the Reynolds number is increased. This effect is manifested whether or not a phase transformation occurs, but it is more notable for the classical Rayleigh–Taylor problem. For $Re > 1$, this effect is magnified: for the problem with a phase transformation, the maximum growth rate for phase transformation problem changes slightly from 0.04356 to 0.04387 when the Reynolds number changes from 1 to 100. Again, consistent with analytical expectations, the range of unstable wavenumbers is not affected by Re.

Plots of the growth rate ω versus the wavenumber k for $At = 0.5$, $Fr = 0.1$, $Re = 1$, and various values of We are shown in figure 9. These plots show that the range of unstable modes and the maximum growth rate both decreases as We is decreased and, thus, exhibit the stabilizing influence of interfacial tension.

4.2. *Influence of the effective viscosity*

Along with the kinematical viscosity ν of the bulk phases, we now consider the influence of the effective viscosity $\alpha + \lambda/2$ of the interface on the stability of the base state. In so doing, we neglect the migrational viscosities κ and β of the interface. In

https://doi.org/10.1017/S002211200600067X Published online by Cambridge University Press

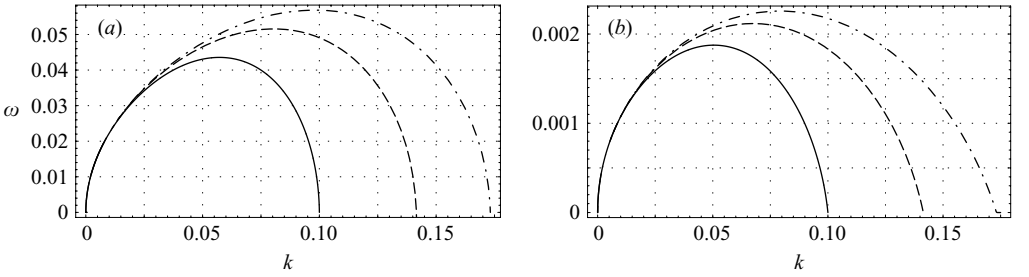


FIGURE 9. Comparison of the relation for the growth rate ω versus the wavenumber k for different Weber numbers We: (a) phase transformation; (b) no phase transformation. $At = 0.05$; $Fr = 1$; $Re = 1$; —, $We = 0.1$; - - -, 0.2; –·–, 0.3.

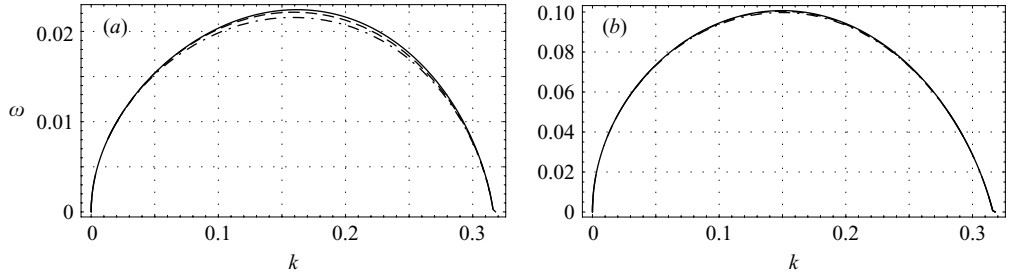


FIGURE 10. Comparison of the relation for the growth rate ω versus the wavenumber k for different Boussinesq number Bo: (a) phase transformation; (b) no phase transformation. $At = 0.5$; $Re = 1$; $We = 0.1$; $Fr = 1$; —, $Bo = 0$; - - -, 10; –·–, 100.

this case $Vo \to \infty$, $Gu \to \infty$, and the dispersion relation (4.12) becomes

$$\omega\left\{\omega^2 + \frac{4|At|k^2\omega}{Re} - \frac{4At^2k^3(q-k)}{Re^2} + \frac{k}{Fr}\left(\frac{k^2}{2We} - At\right)\right\} + \frac{|At|Bok^2}{Re}\left\{q\omega^2 + \left(\frac{k^2}{2We} - At\right)\frac{k}{Fr}(q-k)\right\} = 0, \quad (4.18)$$

which should be compared with the dispersion relation (4.14) for the classical Rayleigh–Taylor problem. Setting $\omega = 0$ in both (4.18) and (4.14), we find that the cutoff wavenumber below which perturbations are unstable is identical for the problems with and without a phase transformation and again given by $k_c = \sqrt{2At\,We}$. Thus, accounting for the dilatational and shear viscosities of the interface does not influence the range of unstable wavenumbers. Next, when $At < 0$, the terms associated with Bo are positive in both (4.18) and (4.14). Arguing as in the case when only the kinematical viscosities of the phases are taken into account, we therefore find that instability is possible only when the phase with the higher density is above that with the lower density.

For small At, the effect of varying Bo is not very significant. To make the effects of Bo discernible, we therefore choose a relatively large value of At. Specifically, for $At = 0.5$, $Re = 1$, $We = 0.1$, $Fr = 1$, and various values of Bo, figure 10 shows plots of the growth rate ω versus the wavenumber k. These plots show that a phase interface is slightly more susceptible to the influence of the effective viscosity $\alpha + \lambda/2$. Consistent with intuitive expectations, the role of effective viscosity is to dissipate the energy of the disturbance and thereby decrease the magnitude of the growth rate corresponding to any unstable mode.

https://doi.org/10.1017/S002211200600067X Published online by Cambridge University Press

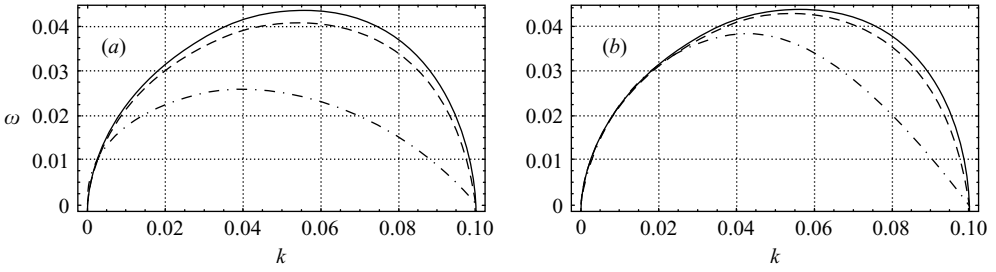


FIGURE 11. Comparison of the relation for the growth rate ω versus the wavenumber k for different Vo and Gu: (*a*) different Vo ($Gu \to \infty$); (*b*) different Gu ($Vo \to \infty$). $At = 0.05$; $Re = 1$; $We = 0.1$; $Fr = 1$; —, $Vo \to \infty$, $Gu \to \infty$; - - -, $Vo = 100$, $Gu = 1$; –·–, 10, 0.1.

4.3. *Influence of the migrational viscosities*

Along with the kinematical viscosity ν of the bulk phases, we now consider the influence of the migrational viscosities κ and β of the interface on the stability of the base state. In so doing, we neglect the effective viscosity $\alpha + \lambda/2$ of the interface. In this case $Bo = 0$ and the dispersion relation (4.12) can be expressed as

$$\left\{2q + \left(\frac{1}{Vo} + \frac{k^2}{Gu}\right)k(q-k)\right\}\left\{\omega^2 + \frac{4|At|k^2\omega}{Re} - \frac{4At^2k^3(q-k)}{Re^2} + \left(\frac{k^2}{2We} - At\right)\frac{k}{Fr}\right\} + \left\{\frac{1}{Vo} + \frac{k^2}{Gu}\right\}\frac{(1-At^2)kq\omega^2}{At^2} = 0. \quad (4.19)$$

Setting $\omega = 0$ in (4.19) shows, once again, that the cutoff wavenumber below which perturbations are unstable is $k_c = \sqrt{2At\,We}$. Also, since the second term on the right-hand side of (4.19) is non-negative and the remaining term involves the product of a non-negative factor with the term appearing on the left-hand side of the dispersion relation (4.15), we may conclude as before that instability is possible only when the phase with the higher density is above that with the lower density.

Plots of the growth rate ω versus the wavenumber k, for $At = 0.05$, $Re = 1$, $We = 0.1$, $Fr = 1$, and various choices of Vo and Gu are provided in figure 11. The plots confirm that, like the shear and dilational viscosities, the migrational viscosities of the interface exert a stabilizing influence.

5. Summary

As is the case for the classical Rayleigh–Taylor problem, our analysis shows that a liquid–liquid phase interface is unstable only when the phase with the higher density is above that with the lower density. When the viscosities of the phases and the interface are neglected, we find that the presence of mass transport in the base state decreases the growth rate of any unstable perturbation. The Atwood number At, Weber number We, and the Froude number Fr play the same roles as they do for the classical Rayleigh–Taylor problem. Specifically, larger At and We lead to a more unstable system while increase in Fr tends to stabilize the system. In the viscous case, we assume that the kinematical viscosities of the phases are equal. We also neglect mass transport in the base state. When the various interfacial viscosities are neglected, we find that the growth rate of unstable modes increases with the Reynolds number Re. The Weber number We and Froude number Fr play the same roles for inviscid and viscous fluids. The range of unstable modes is insensitive to

https://doi.org/10.1017/S002211200600067X Published online by Cambridge University Press

variations of these numbers. However, the growth rates of unstable modes increase and decrease, respectively, when *We* and *Fr* are increased. When the migrational viscosities of the interface are neglected, but the dilational and shear viscosities of the interface are taken into account, we find that the associated Boussinesq number *Bo* does not affect the range of unstable modes, but diminishes slightly the growth rate of unstable modes. When the dilatational viscosity of the interface is neglected, but the migrational viscosities of the interface are taken into account, we find that the roles of the associated dimensionless parameters, the Voronkov number *Vo* and the Gurtin number, *Gu* are very similar to that of *Bo*. However, while they do not alter the interval of unstable modes, their impact on the growth rate is more significant.

Following Taylor (1950), our framework can be extended to show that the gravitationally unstable arrangement, when the phase with the higher density is above that with the lower density, is stabilized by acceleration in the direction of gravity.

We leave for a future work the question of how viscosity influences the stability of base states involving mass transport. Also, a more comprehensive study of the instability of a liquid–liquid phase interface would generally require the consideration of a finite system with bounding surfaces and, perhaps, contact lines. The inclusion of bounding surfaces requires extra boundary conditions (Elgowainy & Ashgriz 1997) and the assumption of exponentially decaying velocity and pressure field in the perpendicular direction would not be valid. Consequently, an algebraic dispersion relation like (4.12) might not exist and partial differential equations requiring numerical simulation would most probably arise. To account for contact lines, it would be necessary to extend the theory developed by Anderson *et al.* (2005) in the manner discussed by Gurtin (2000). Moreover, different results might be expected if either the bulk extra stress (1.5) or the interfacial extra stress (1.8) were non-Newtonian.

Finally, we hope that the stability results presented here will lead to experimental tests in systems such as those considered by Aasland & McMillan (1994), Togaya (1997), Glosli & Ree (1999), and Katayama *et al.* (2000).

This work was supported by the U S Department of Energy. We thank Bill Phillips and Oleg Chkliaev for very helpful discussions and suggestions.

REFERENCES

Aasland, S. & McMillan, P. F. 1994 Density-driven liquid–liquid phase seperation in the system Al_2O_3–Y_2O_3. *Nature* **369**, 633–636.

Anderson, D. M., Cermelli, P., Fried, E., Gurtin, M. E. & McFadden, G. B. 2006 General dynamical sharp-interface conditions for phase transformations in heat-conducting fluids. *J. Fluid Mech.* (in press).

Angell, C. A. 1995 Formation of glasses from liquids and biopolymers. *Science* **267**, 1924–1935.

Bellman, R. & Pennington, R. H. 1954 Effects of surface tension and viscosity on Taylor stability. *Q. Appl. Maths* **12**, 151–162.

Boussinesq, M. J. 1913 Sur l'éxistance d'une viscosité superficielle, dans la mince couche de transition separant un liquide d'une autre fluide contique. *Ann. Chim. Phys.* **29**, 349–357.

Burghardt, A. & Bartelmus, G. 1994 Condensation of vapour mixtures forming two immiscible liquid phases. *Inz. Chemiczna Proces.* **15**, 327–351.

Chandrasekhar, S. 1955 The character of the equilibrium of an incompressible heavy viscous fluid of variable density. *Proc. Camb. Phil. Soc.* **51**, 162–178.

Chandrasekhar, S. 1961 *Hydrodynamic and Hydromagnetic Stability*. Dover.

Daly, B. J. 1967 Numerical study of two fluid Rayleigh–Taylor instability. *Phys. Fluids* **10**, 297–307.

Drazin, P. G., & Reid, W. H. 2004 *Hydrodynamic Stability*. Cambridge University Press.

https://doi.org/10.1017/S002211200600067X Published online by Cambridge University Press

Elgowainy, A. & Ashgriz, N. 1997 The Rayleigh–Taylor instability of viscous fluid layers. *Phys. Fluids* **9**, 1635–1649.

Galenko, P. K. & Danilov, D. A. 2004 Linear morphological stability analysis of the solid-liquid interface in rapid solidification of a binary system. *Phys. Rev.* E **69**, 051608.

Glosli, J. N. & Ree, F. H. 1999 liquid–liquid phase transformation in carbon. *Phys. Rev. Lett.* **82**, 4659–4662.

Gurtin, M. E. 2000 *Configurational Forces as Basic Concepts of Continuum Physics*. Springer.

Gurtin, M. E. & Struthers, A. 1990 Multiphase thermomechanics with interfacial structure 3. Evolving phase boundaries in the presence of bulk deformation. *Arch. Rat. Mech. Anal.* **112**, 97–160.

Hertz, H. 1882 Ueber die Verdunstung der Flssigkeiten, insbesondere des Quecksilbers, im luftleeren Raume. *Ann. Phys.* (*Leipzig*) **17**, 177–200.

Higuera, F. J. 1987 The hydrodynamic stability of an evapourating liquid. *Phys. Fluids* **3**, 679–686.

Hsieh, D. Y. 1978 Interfacial stability with mass and heat transfer. *Phys. Fluids* **21**, 745–748.

Katayama, Y., Mizutani, T., Utsumi, W., Shimomura, O., Yamakata, M. & Funakoshi, K. 2000 A first-order liquid–liquid phase transition in phosphorus. *Nature* **403**, 170–173.

Knudsen, H. 1915 Die Maximale Verdampfungsgeschwindigkeit des Quecksilbers. *Ann. Phys.* (*Leipzig*) **47**, 697–708.

Kurita, R. & Tanaka, H. 2005 On the abundance and general nature of the liquid–liquid phase transition in molecular systems. *J. Phys.–Condens. Matter* **17**, 293–302.

Langmuir, I. 1916 The evapouration, condensation and reflection of molecules and the mechanism of adsorption. *Phys. Rev.* **8**, 149–176.

Lee, H. K. & Swendsen, R. H. 2001 Simple model of liquid–liquid phase transitions. *Phys. Rev.* B **64**, 214102.

Lewis, D. J. 1950 The instability of liquid surfaces when accelerated in a direction perpendicular to their planes. II *Proc. R. Soc. Lond* A **202**, 81–96.

Mullins, W. W. & Sekerka, R. F. 1963 Morphological stability of a particle growing by diffusion or heat flow. *J. Appl. Phys.* **34**, 323–329.

Plesset, M. S. & Prosperetti, A. 1982 Reply to comments on 'General analysis of stability of superposed fluids.' *Phys. Fluids* **25**, 911–912.

Rayleigh, Lord 1900 Investigation of the character of the equilibrium of an incompressible heavy fluid of variable density. *Scientific Papers II*, 200.

Rzehak, R., Müller-Krumbhaar, H. & Marquardt, W. 2003 liquid–liquid phase transition in flow systems. *Chem. Engng Sci.* **58**, 247–255.

Scriven, L. E. 1960 Dynamics of a fluid interface. *Chem. Engng Sci.* **12**, 98–108.

Siegert, M., Stichlmair, J., Repke, J. U. & Wozny, G. 2000 Heterogeneous azeotropic distillation in packed columns: experimental results. *Chem. Engng Technol.* **23**, 1047–1050.

Tanaka, H. 2000 General view of a liquid–liquid phase transition. *Phys. Rev.* E **62**, 6968–6976.

Taylor, G. I. 1950 The instability of liquid surfaces when accelerated in a direction perpendicular to their planes. *Proc. R. Soc. Lond.* A **201**, 192–196.

Togaya, M. 1997 Pressure dependence of the melting temperature of graphite and the electrical resistivity of liquid carbon. *Phys. Rev. Lett.* **79**, 2474–2477.

Trivedi, R. & Kurz, W. 1986 Morphological stability of a planar interface under rapid solidification conditions. *Acta Metall.* **34**, 1663–1670.

Troniewski, L., Filipczak, G., Witczak, W. & Trembacz, J. 2001 Boiling of immiscible liquid mixtures. *Inz. Chemiczna Proces.* **22**, 1411–1416.

Volmer, M. 1939 *Kinetik der Phasenbildung*. T. Steinkopff, Dresden.

Voronkov, V. V. 1964 Conditions for formation of mosaic structure on a crystallization front. *Sov. Phys. Solid State* **6**, 2378–2381.

Widagdo, S. & Seider, W. D. 1996 Azeotropic distillation. *AICHE J.* **42**, 96–130.

https://doi.org/10.1017/S002211200600067X Published online by Cambridge University Press